

Supplementary Information

“Contact Chemistry and Single Molecule Conductance: A Comparison of Phosphines, Methyl Sulfides and Amines”

Young S. Park^{1,3}, Adam C. Whalley^{1,3}, Maria Kamenetska^{2,3}, Michael L. Steigerwald¹, Mark S. Hybertsen^{3,4}, Colin Nuckolls^{1,3}, Latha Venkataraman^{2,3}

¹Department of Chemistry

²Department of Applied Physics and Applied Mathematics

³Center for Electron Transport in Molecular Nanostructures, Columbia University, New York, New York

⁴Center for Functional Nanomaterials, Brookhaven National Labs, Upton, New York

Content:

Synthetic Procedure

Measurements and Data Analysis

Theoretical Procedure

References

Synthetic Procedures:

Starting materials and reagents were obtained from commercial sources or synthesized by procedures noted below.

Compound 1:

1,4-Bis(dimethylphosphino)butane was prepared from 1,4-dibromobutane by the method described for 1,6-bis(dimethylphosphino)hexane and 1,8-bis(dimethylphosphino)octane by Gin.¹ ¹H NMR (300MHz, CDCl₃) δ 0.99 (s, 12H), 1.41 (m, 8H). ¹³C NMR (75MHz, CDCl₃) δ 14.40 (d, *J* = 12.5Hz), 27.82 (m), 32.14 (d, *J* = 8.9Hz). ³¹P NMR (CDCl₃, 121MHz) δ -51.66.

Compound 2:

1,6-Bis(dimethylphosphino)hexane was prepared as previously described.¹

Compound 3:

1,8-Bis(dimethylphosphino)octane was prepared as previously described.¹

General procedure for compound **4**, **5** and **6**(modified from reference²).

To a suspension of sodium thiomethoxide(2.10g, 0.030mmol) in ethanol(100mL) was added dibromoalkane(0.010mmol), and the reaction mixture was refluxed overnight with stirring. The resulting mixture was concentrated in vacuo, poured into water(300mL), and steam-distilled. The product was extracted with dichloromethane(3x100mL) and the combined organic layer was dried over magnesium sulfate anhydrous. After removal of solvent in vacuo, the compound was purified using column chromatography, yielding a colorless liquid.

Compound 4:

1,2-Bis(methylthio)ethane

$^1\text{H NMR}$ (300MHz, CDCl_3) δ 2.72(s, 4H), 2.14(s, 6H).

Compound 5:

1,4-Bis(methylthio)butane

$^1\text{H NMR}$ (300MHz, CDCl_3) δ 2.52(m, 4H), 2.11(s, 6H), 1.72(m, 4H).

Compound 6:

1,7-Bis(methylthio)heptane

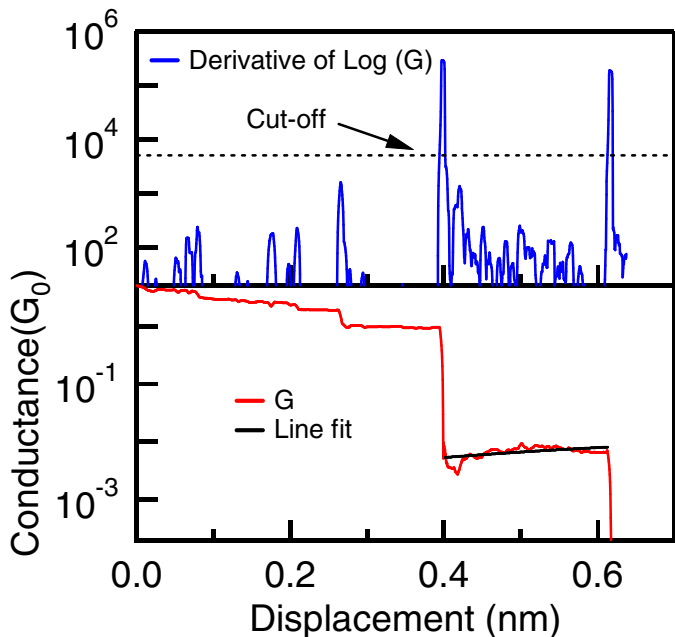
$^1\text{H NMR}$ (300MHz, CDCl_3) δ 2.49(t, $J = 7.5\text{Hz}$, 4H), 2.10(s, 6H), 1.60(m, 4H), 1.37(m, 6H).

Measurement and Data Analysis:

The details of our experimental apparatus has been described previously^{3,4}. Briefly, the STM was constructed from a home-built tip holder mounted on top of a single-axis piezoelectric positioner (Mad City Labs). A bias was applied between a cut Au wire tip and an Au substrate placed on top of the piezoelectric positioner and the resulting current was converted to a voltage with a current amplifier (Keithley 428). Data collection and control of the piezoelectric positioner were done by means of a data acquisition board (National Instruments, PXI-4461) driven by a customized program using Igor software (Wavemetrics Inc.) For the conductance trace measurements, the substrate approached the tip until a set conductance larger than G_0 was measured to ensure that the Au/molecule/Au junction from the previous measurement was completely destroyed. The sample was then withdrawn at a rate of 20 nm/s and the current and position data was recorded at a 40 kHz sampling frequency. Histograms were constructed from the current versus position traces by converting currents to conductances and binning the data as a function of conductance. For step length measurements, the custom piezoelectric positioner has a built in position sensor calibrated by the manufacturer, which has sub-angstrom accuracy. In addition, we have calibrated the piezo using interference measurements, and find the absolute values of the measured displacements to be accurate to within 5%.

The molecular junction step lengths were determined by an automated fitting algorithm. First, a Lorentzian was fit to the histograms computed from all measured traces to determine a molecular conductance peak position (G_{peak}) and the full width at half maximum for the peak (G_{width}). For each measured trace, the derivative of the logarithm of the trace was computed. Traces with peaks in the derivative that crossed a threshold of 5000 were considered further. The average conductance from the raw data in the region between two successive peaks was computed. (See Supplementary Figure 1). Traces were considered to have molecular steps if this average conductance was within $G_{\text{peak}} \pm G_{\text{width}}$ and if this region had more than 5 data points. Steps that had fewer than 5 data points, or equivalently those that were shorter than 0.007 nm were not included in the analysis. The step length was then defined to be the length of the region between the two peaks in the derivative traces. If traces had multiple steps within the same conductance region, the sum of the lengths of the individual steps was used as a total step length. However, the distribution of step lengths for traces with single steps (which accounts for more than

75% of the traces with steps) is the same as the distribution of total step lengths for steps that have an average conductance within $G_{\text{peak}} \pm G_{\text{width}}$.



Supplementary Figure 1: A sample conductance trace (lower panel) and the derivative of the log of the traces (upper panel).

Theoretical Procedures:

The generalized gradient approximation (GGA) as formulated by Perdew, Burke and Ernzerhof (PBE) was used.⁵ The molecular calculations were done with Jaguar v5.0⁶ using a 6-31g** basis for the light atoms and a lacvp** basis for Au.⁷ The molecular geometry was fully relaxed. Each X-Au link was modeled using Au clusters ranging from a single atom up to five atoms. The key features do not depend on the choice of cluster, although we find that the binding energy to fcc fragments is generally lower than binding to fully relaxed Au clusters (which tend not to have an fcc derived structure for less than 20 Au atoms⁸). To simulate an undercoordinated Au contact atom on a close-packed Au contact, we focus on the model in Figure 3D with four Au atoms frozen in a fragment of the fcc packing arrangement from metallic Au and an unconstrained Au atom initially located in the environment of an hcp hollow site on an Au(111) facet. The junction elongation process is modeled by separating the frozen Au atoms representing the tip and substrate in 0.2 Å steps, allowing all other atoms to relax fully. The force applied to maintain the junction separation is the derivative of the junction energy with respect to separation. Although not explicitly included in the data in Fig. 3, we estimate that basis set superposition error leads to an overestimate in the maximum force on the junction in Fig. 3 by less than 10%.

Using the Au5 clusters to simulate the tip and substrate, the initial position of the clusters defines a z-axis perpendicular to the triangle defining the hollow sites. The centers of the

hollow sites are displaced along $\pm y$ by 0.8 Å. The backbone of the butane is initially slightly tilted with respect to the z-axis (about 20 degrees). The overall structure has C_{2h} symmetry for NH₂ and PMe₂ and C_i symmetry for SMe. At equilibrium, the X-Au bond forms with an estimated energy of 0.7 eV (NH₂), 0.6 eV (SMe), and 1.2 eV (PMe₂) and a bond length of 2.21 Å (NH₂), 2.45 Å (SMe) and 2.35 Å (PMe₂). The contact Au atom remains near the center of the hollow site. The maximum force sustained by the junction is 1.0 nN (NH₂), 0.8 nN (SMe), and 1.4 nN (PMe₂). Sampling other initial structures, the maximum force varies at the level of 0.1-0.2 nN with details such as the initial tilt angle of the backbone relative to the direction of elongation.

Reference:

1. Pindzola, B. A.; Jin, J. Z.; Gin, D. L., Cross-linked normal hexagonal and bicontinuous cubic assemblies via polymerizable gemini amphiphiles. *Journal of the American Chemical Society* **2003**, 125, (10), 2940-2949.
2. Anklam, E., Synthesis of Alpha-Halogeno-Omega-Alkylthioalkanes and Alpha,Omega-Bisalkylthioalkanes. *Synthesis-Stuttgart* **1987**, (9), 841-843.
3. Ulrich, J.; Esrail, D.; Pontius, W.; Venkataraman, L.; Millar, D.; Doerrer, L. H., Variability of Conductance in Molecular Junctions. *Journal of Physical Chemistry B* **2006**, 110, (6), 2462-2466.
4. Venkataraman, L.; Klare, J. E.; Tam, I. W.; Nuckolls, C.; Hybertsen, M. S.; Steigerwald, M. L., Single-Molecule Circuits with Well-Defined Molecular Conductance. *Nano Letters* **2006**, 6, (3), 458 - 462.
5. Perdew, J. P.; Burke, K.; Ernzerhof, M., Generalized gradient approximation made simple. *Physical Review Letters* **1996**, 77, (18), 3865-3868.
6. Jaguar Jaguar 5.0; Schrodinger, L.L.C., Portland, OR, 1991-2003.
7. Wadt, W. R.; Hay, P. J., Abinitio Effective Core Potentials for Molecular Calculations - Potentials for Main Group Elements Na to Bi. *Journal of Chemical Physics* **1985**, 82, (1), 284-298.
8. Wang, J. L.; Wang, G. H.; Zhao, J. J., Density-functional study of Au-n(n=2-20) clusters: Lowest-energy structures and electronic properties. *Physical Review B* **2002**, 66, (3), 035418.